BJR

https://doi.org/10.1259/bjr.20180129

Received: 31 January 2018 | Revised: 27 March 2018 | Accepted: 30 March 2018

Cite this article as:
Bayramoglu Z, Caliskan E, Karakas Z, Karaman S, Tugcu D, Somer A, et al. Diagnostic performances of superb microvascular imaging, shear wave elastography and shape index in pediatric lymph nodes categorization: a comparative study. *Br J Radiol* 2018; **91**: 20180129.

FULL PAPER

Diagnostic performances of superb microvascular imaging, shear wave elastography and shape index in pediatric lymph nodes categorization: a comparative study

[1]ZUHAL BAYRAMOGLU, [1]EMINE CALISKAN, [2,3]ZEYNEP KARAKAS, [2,3]SERAP KARAMAN, [2,3]DENIZ TUGCU, [4]AYPER SOMER, [4]MANOLYA ACAR, [5,6]FERHAN AKICI and [1]IBRAHIM ADALETLI

[1]Department of Radiology, Istanbul Faculty of Medicine, Istanbul University, Istanbul, Turkey
[2]Department of Pediatric Hematology, Istanbul Faculty of Medicine, Istanbul University, Istanbul, Turkey
[3]Department of Oncology, Istanbul Faculty of Medicine, Istanbul University, Istanbul, Turkey
[4]Department of Pediatric Infectious Diseases, Istanbul Faculty of Medicine, Istanbul University, Istanbul, Turkey
[5]Department of Pediatric Hematology, Kanuni Sultan Suleyman Training and Research Hospital, Istanbul, Turkey
[6]Department of Oncology, Kanuni Sultan Suleyman Training and Research Hospital, Istanbul, Turkey

Address correspondence to: Zuhal Bayramoglu
E-mail: *incezuhal@yahoo.com*

Objective: To determine the diagnostic utility of a vascularity index via superb microvascular imaging in lymph nodes of children with malignant lymphoma and acute lymphadenitis compared to normal lymph nodes.
Methods: We performed a retrospective study for multiparametric lymph node (LN) evaluation. Malignant lymphoma diagnosed via histopathological examination and lymph nodes receiving an acute lymphadenitis diagnosis based on clinical and laboratory findings constituted the study subgroups. We calculated a shape index [SI (percent of shortest to longest diameter)] using gray-scale ultrasonography and elasticity and velocity values via shear wave elastography (SWE) as well as a vascularity index (VI) using superb microvascular imaging (SMI) for comparison with normal lymph nodes.
Results: 45 lymph nodes diagnosed with malignant lymphoma, 72 lymph nodes diagnosed with acute lymphadenitis and 146 normal lymph nodes were evaluated. For differentiating lymphoma from normal lymph nodes, vascularity index cut-off values higher than 15% represented a diagnostic accuracy of 95%; cut-off elasticity values higher than 17 kPa exhibited a diagnostic accuracy of 99%. Optimal VI, elasticity, velocity and SI cut-off values in differentiating lymphoma from lymphadenitis were 15%, 17 kPa, 2.45 m sn^{-1} ($p < 0.001$) and 65% ($p < 0.002$) with calculated diagnostic accuracies of 83, 87, 88 and 68%, respectively.
Conclusion: Vascularity index values obtained via superb microvascular imaging and SWE would be reasonably useful in differentiating malignant lymphoma and acute lymphadenitis from normal LNs. SWE would be more efficient in distinguishing malignant lymph nodes from acute lymphadenitis compared with superb microvascular imaging.
Advances in knowledge: Vascularity index by superb microvascular imaging would be a novel Doppler parameter in differentiating both lymphoma from lymphadenitis and also lymphadenitis from normal lymph nodes.

INTRODUCTION

Doppler ultrasound evaluation would be a complementary modality by demonstrating hilar and peripheral vascular branches in an enlarged lymph node (LN) when lymphadenitis is considered or suspected of neo-vascularization due to the presence of lymphoma. Several studies have evaluated the advantages of resistive and pulsatility indices for identifying malignant LNs.[1] Because benign and malignant conditions could overlap with each other, these indices exhibit a limited role in determining malignant LNs. Superb microvascular imaging (SMI) is an advanced Doppler modality that provides a great deal of data regarding the intralesional vascular network with vessel branches, especially in hypervascular conditions. Higher diagnostic performance of SMI when compared to color and Power Doppler has been reported in pediatric testicular tissue, thyroid glands and gastrointestinal disorders and breast masses.[2–5] By suppressing scattering and demonstrating signals of low-velocity flows based on the ability to distinguish motion artifacts from slow-velocity signals, tiny vessels can be clearly detected by SMI. The vascularity index (VI) is a novel Doppler parameter that

can be calculated using an automatized application that allows for quantification of the signals by providing the ratio of colored pixels to all pixels within the region of interest (ROI). As far as we know, no previous study has investigated the VI differences among lymphadenitis and lymphoma, which is a common problem in management of the patients presented with enlarged LNs.

Because increased stiffness is expected for malignant tissues, shear wave elastography (SWE) has been reported as a promising modality for determining lymphoma. Quantitative real-time SWE is a novel imaging modality that provides contributions regarding viscoelastic tissue properties by performing a higher intensity pulse that is transmitted to produce shear waves, extending laterally from the target tissue and then tracked with low-intensity pulses to find the shear velocity related to Young's modulus. A few studies have been published concerning ultrasound elastography for determining malignant lymphoma and present diagnostic accuracies between 89 and 93%.[6–10] As far as we know, no comparative study regarding quantitative SWE investigating malignant lymphoma and lymphadenitis has been conducted.

The main objective of this study was to reveal diagnostic performances of the VI via SMI, SWE and the shape index (SI) in lymphadenitis and lymphoma.

METHODS AND MATERIALS

Patient selection

This study was retrospectively designed and collected at the Istanbul Faculty of Medicine after approval was obtained from the local ethics committee and informed consent was obtained from the parents of the participants between September 2016 and December 2017. Totally, 263 LNs were evaluated in 104 subjects including the study and control groups. The study group included 45 LNs of 15 consecutive patients diagnosed with malignant lymphoma via histopathological examination and 72 LNs of 36 consecutive patients finally diagnosed with acute lymphadenitis based on clinical parameters such as fever, pain and rapid enlargement as well as laboratory parameters such as increased white blood cell count, C-reactive protein, sedimentation or viral antibodies. The remaining 146 LNs, which are normal on ultrasonography in terms of size, shape and cortical echogenicity and under follow-up for at least 8 months without enlargement and are commonly located in the cervical lymphatic stations of 53 healthy patients, were included in the control group. Clinical examinations of the patients were normal and, there was no laboratory finding suggesting infection and their total blood count were within the normal range. The malignant LNs were diagnosed with ultrasound-guided percutaneous tru-cut biopsy with 18 G needle in eight patients and excisional biopsy in seven patients who subsequently underwent chemotheraphy. The patients with lymphadenitis were treated with antibiotics and followed-up for at least 6 months to confirm the healing of the lymphadenopathy. All LNs in the control group and both study subgroups underwent grayscale ultrasonography, SMI and SWE examinations.

Grayscale and Doppler ultrasound evaluation

Ultrasound assessments were performed through consensus of two radiologists having more than 7 years of ultrasonography experience using a 14 MHz linear array transducer (Canon Aplio 500 Platinium; Japan). All examinations were performed in a supine position with a hyperextended neck, and the patient's head was turned away from the site of examination. We recorded three diameters of the LNs and calculated volumes with an automated formula (length × width × depth × 0.52). We evaluated the shape, SI, capsular irregularity, echogenicity of the cortex and visualization of the hilar fatty tissue. LNs exhibiting any of the findings including spherical shape, being hypoechogenic than the muscles, obliterated fatty hilum, reticular pattern[11] and/or increased peripheral vascularity on color Doppler ultrasound evaluation were indications for histopathological verification. Malignant LNs obtained in any lymphatic station and normal LNs, particularly located in bilateral jugulodigastric and anterior cervical LN stations, were examined. The patients were asked to remain still during vascular imaging. The evaluation of the lymph nodes were blinded to clinical and laboratory data and prior to the histopathological evaluation. We excluded LNs with abscess formation in the lymphadenitis group that were finally diagnosed as either viral or non-specific bacterial lymphadenitis. Enlarged LNs in the study group and bilateral normal jugulodigastric and prominent anterior cervical LNs within the control group were examined.

Superb microvascular imaging

SMI is a novel Doppler imaging modality that substracts flow signals displayed as color or as a monochrome image using high frame rates (>50 Hz) and lower pulse repetition frequencies (220–234 Hz) than power Doppler imaging (10–15 Hz *vs* 870–966 Hz, respectively). SMI was performed by two radiologists having at least 7 years of Doppler ultrasound experience using a 14 MHz linear array transducer (Canon Aplio 500 Platinium; Japan) with a pulse repetition frequency of 150–180 Hz. Once the longitudinal plan and the hilum of the LNs were exhibited clearly, then the SMI assessment was performed. The margins of each LN were manually outlined on selected SMI images to represent ROI, and a quantitative evaluation of VI of LNs via SMI was achieved after grayscale pixels within the outlined area were automatically eliminated by an algorithm. The percentage of colored pixels to the total pixel numbers within the ROI represents VI (Figure 1a–c). The mean value of the VI for each LN was calculated from three measurements of each node obtained from longitudinal views.

Shear wave elastography

Two radiologists having more than 10 and 2 years of SWE experience performed the examination by consensus. The real-time synchrone propagation and shear wave map were demonstrated on the longitudinal plan of all LNs, and we waited for smooth and parallel propagation lines. The elasticity range was set to 0–80 kPa, and the velocity range was set to 0–6 m sn^{-1}. We selected three round-shaped ROIs within the stiffest portion of the LN cortex measuring 4 mm in diameter (Figure 2a–c) and repeated for five times. Mean elasticity (kPa) and velocity (m s^{-1}) values were automatically calculated by averaging 15 values for each LN.

Figure 1. Examples of LN stiffness measurement using ultrasound SWE. The circles indicating the ROI were placed in the stiffest portion of the LN cortex. The values measured were shown at the bottom. (a) Normal jugulodigastric LN of an asymptomatic 5-year-old male patient. (b) Lymphadenitis in an 8-year-old female patient. (c) Level 4 cervical LN diagnosed with Hodgkin lymphoma in an 11-year-old male patient. LN; lymph node; ROI; region of interest; SWE, shear wave elastography.

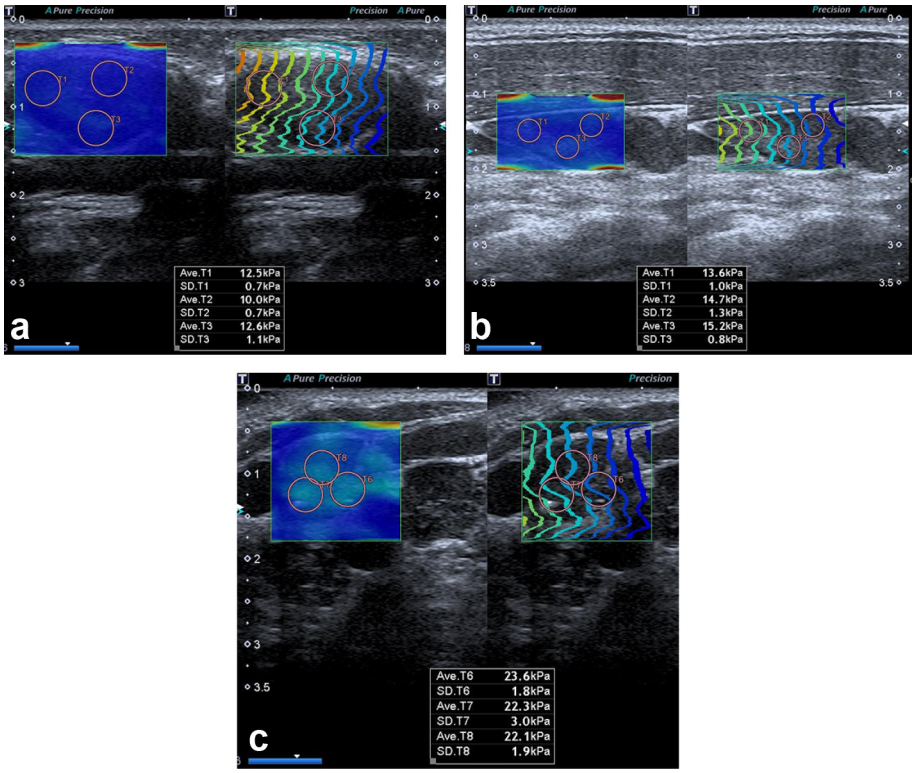

Statistical analysis

Statistical analysis was performed using SPSS (v. 21.0, SPSS Inc.). The normality of the distribution of the quantitative data were checked using the Kolmogorov-Smirnov test. Categorical variables were demonstrated as percentages. Descriptive analysis of quantitative variables such as age of the patients, volume of the LNs, elasticity and velocity values, VI and SI values were expressed as mean ± standard deviation (SD) or median with range (minimum–maximum).

VI and elasticity parameters were compared among normal LNs, acute lymphadenitis and malignant lymphoma. Kruskal–Wallis and Mann–Whitney *U* tests were used to compare independent groups. Spearman's correlation analysis was performed to evaluate the relationship between elasticity parameters and VI with each patient's age, LN volumes, diameters and SI. A p value < 0.05 was considered statistically significant.

The diagnostic utility of VI by SMI for estimating lymphoma and lymphadenitis was evaluated using receiver operating characteristic (ROC) curve analysis. The diagnostic accuracy of VI by SMI and the elasticity parameters by SWE and SI as a quantitative grayscale ultrasonography parameter were provided by calculating the area under the ROC curve. We presented optimal cut-off values with sensitivity, specificity, positive predictive value (PPV), negative predictive value (NPV) and diagnostic accuracy. A p value < 0.05 designated statistical significance.

RESULTS

Categorical variables by frequency

The 263 lymph nodes (normal, n = 146; lymphadenitis, n = 72; lymphoma, n = 45) from 104 patients (55 males, 49 females; mean age ± SD; 10.5 ± 3.5 years old; age range, 2–18 years), in which the final diagnosis was achieved, were investigated. Commonly encountered prominent normal LNs were found in the level 2 and 1b cervical lymphatic stations. Peripheral vascularity was found in 0% of the normal LNs, in 10% of the lymphadenitis and in 93% of the malignant LNs.

Continuous variables: descriptive statistics and *t* test

Descriptive statistics regarding the continuous variables of the LNs are provided in Table 1. No statistically significant difference was found among mean ages of participants within lymphadenitis, lymphoma and the control group (10.7 ± 3.6, 11.7 ± 4.3 and 11.8 ± 3.6, respectively, $p > 0.05$).

Median VI with range in the lymphoma, lymphadenitis and control groups were 17.85 (7–36)%, 14.86 (1–24)% and 4.72 (0.1–17)%, respectively. There were statistically significant differences among median VI values of the study and control groups ($p < 0.001$) and also when we compared the study subgroups ($p < 0.001$) (Table 2). When we compared the normal jugulodigastric and anterior cervical LNs, the median

Figure 2. Examples of LN VI using superb microvascular imaging. The LNs were outlined and ratio of color pixels to all the pixels within the ROI was automatically calculated as VI. The values measured are shown at the bottom. (a) Normal jugulodigastric LN of asymptomatic 5-year-old male patient. (b) Lymphadenitis in an 8-year-old female patient. (c) Level 2 LN diagnosed with Hodgkin lymphoma in an 11-year-old male patient demonstrating increased peripheral non-uniform disorganized vessels. LN, lymph node; ROI, region of interest; VI, vascularity index.

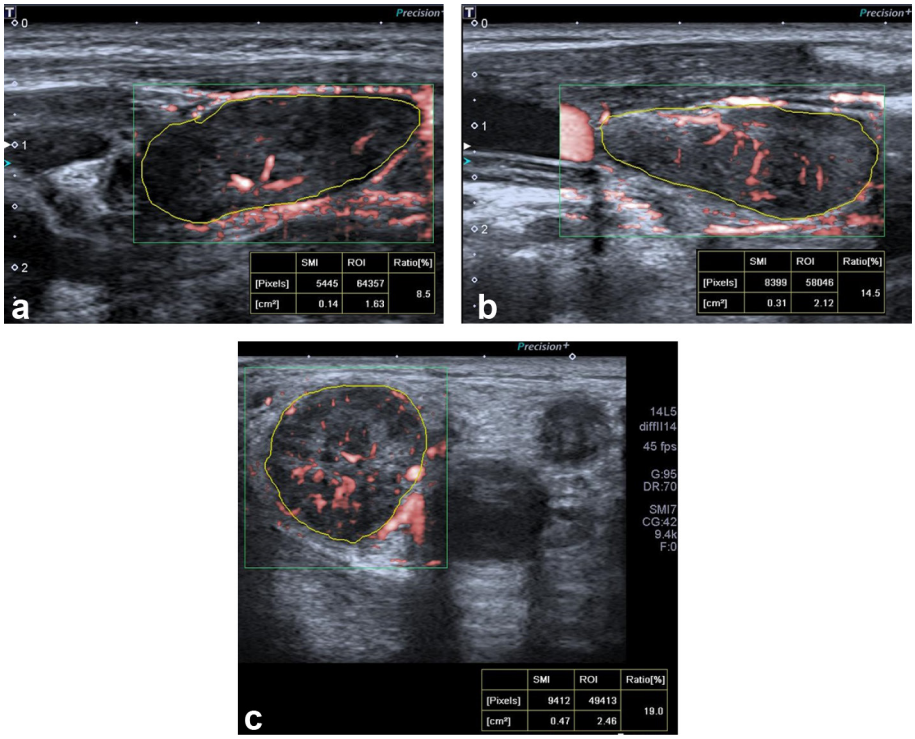

VI value was significantly higher in jugulodigastric LNs (7.9; 2–9% *vs* 3.7; 1.5–5%, $p < 0.001$), but there was not a significant difference in terms of elasticity parameters (jugulodigastric LNs; 11.4; 10–11.7 kPa, 1.94; 1.7–2.01 m sn^{-1} *vs* anterior cervical LNs; 10.5; 9–12.5 kPa, 1.84; 1.72–2.03 m sn^{-1}, respectively, $p > 0.05$).

There were statistically significant differences among median elasticity and velocity values of malignant LNs (24.46;15–45.5 kPa, 2.82; 2.24–3.83 m sn^{-1}), lymphadenitis (13.21; 6.5–28.3 kPa, 2.07; 1.48–3.02 m sn^{-1}) and normal LNs (11.19; 5.9–16.6 kPa, 1.92; 1.42–2.35 m sn^{-1}). Mean elasticity and velocity values were significantly higher in lymphoma than those with lymphadenitis and normal LNs ($p < 0.001$).

There were significant differences among mean LN volumes (excluding normal LNs in jugulodigastric station; 1.78; 0.29–7.96cc in lymphadenitis, 6.83; 0.69–40.2cc in lymphoma and

Table 1. Descriptive statistics; age of the patients along with grayscale ultrasonography, SMI and SWE parameters of the lymph nodes

	Control group (*n*:146)	Lymphadenitis (*n*:72)	Lymphoma (*n*:45)
	Mean ± SD Median (min–max)	Mean ± SD Median (min–max)	Mean ± SD Median (min–max)
Age (years)	11.88 ± 3.69	10.73 ± 3.62	11.72 ± 4.34
Shortest diameter (mm)	7.33 (3–14)	10.57 (5.00–18)	17.87 (8–37)
Longest diameter (mm)	17.84 (10–41)	19.25 (10–37)	26.24 (14–50)
Volume (cc)	1.04 (0.12–7.89)	1.78 (0.29–7.96)	6.83 (0.69–40.24)
Elasticity (kPa)	11.19 (5.9–16.6)	13.21 (6.5–28.3)	24.46 (15–45.5)
Velocity (m sn^{-1})	1.92 (1.42–2.35)	2.07 (1.48–3.02)	2.82 (2.24–3.83)
VI (%)	4.72 (0.1–17)	14.86 (1–24)	17.85 (7–36)
SI (%)	0.42 (0.23–0.63)	0.57 (0.28–1.08)	0.72 (0.31–1.14)

SD, standard deviation; SI, shape index; SMI, superb microvascular imaging; SWE, shear wave elastography; VI, vascularity index.

Table 2. Results of Kruskal–Wallis and Mann–Whitney *U* tests for differences between control, lymphadenitis and lymphoma groups

Test		Variable					
		Volume (cc)	Shortest diameter (mm)	SI (%)	Elasticity (kPa)	Velocity (m sn^{-1})	VI (%)
Kruskal–Wallis		0.001	0.001	0.001	0.001	0.001	0.001
Mann–Whitney *U* test	Control *vs* Lymphadenitis	0.001	0.001	0.001	0.01	0.01	0.001
	Control *vs* Lymphoma	0.001	0.001	0.001	0.001	0.001	0.001
	Lymphadenitis *vs* Lymphoma	0.001	0.001	0.002	0.001	0.001	0.001

SI, shape index; VI, vascularity index.

1.04; 0.12–7.89 cc in the control group, $p < 0.001$). The mean follow-up duration for normal LNs was 10 ± 2 months.

Median SI values were significantly higher in the lymphoma group when compared to the lymphadenitis and control groups (normal LNs, 42; 23–63%; acute lymphadenitis, 57; 28–108% and malignant LNs, 72; 31–114%, $p < 0.002$). Median shortest diameters were significantly higher in the lymphoma group compared with those from the lymphadenitis and normal LN groups (17.87; 8–37 mm, 10.57; 5–18 mm, 7.33; 3–14 mm, $p < 0.001$, respectively).

Diagnostic performance of VI, SWE, SI

Diagnostic performances of VI by SMI, the elasticity parameters and SI are exhibited in Table 3. The optimal cut-off VI value for differentiating lymphadenitis from normal LNs was 11% with sensitivity, specificity, PPV, NPV and a diagnostic accuracy of 85, 84, 85, 85 and 85%, respectively (Figure 3). The optimal cut-off VI value for differentiating lymphoma from normal LNs was 15% with sensitivity, specificity, PPV, NPV and a diagnostic accuracy of 91, 99, 96, 94 and 95%, respectively. The optimal cut-off VI value for differentiating lymphoma from lymphadenitis was 15% with sensitivity, specificity, PPV, NPV and a diagnostic accuracy of 85, 81, 84, 82 and 83%, respectively.

Optimal cut-off elasticity and velocity values were 15 kPa and 2.24 m sn^{-1} for differentiating lymphadenitis from normal LNs with sensitivity, specificity, PPV, NPV and a diagnostic accuracy of 27, 96, 82, 74, 74% and 25 ,97, 82, 73, 74%, respectively. Optimal cut-off values for elasticity and velocity were 17 kPa and 2.45 m sn^{-1} for differentiating lymphoma from normal LNs with sensitivity, specificity, PPV, NPV and a diagnostic accuracy of 96, 100, 100, 99, 99% and 90, 99, 96, 95, 95%, respectively. Optimal cut-off elasticity and velocity values were 17 kPa and 2.45 m sn^{-1} for differentiating lymphoma from lymphadenitis with sensitivity, specificity, PPV, NPV and a diagnostic accuracy of 96, 81, 76, 97% and 96 , 82, 77, 98, 88%, respectively.

Optimal cut-off SI values were >55% for differentiating lymphadenitis from normal LNs and >65% for differentiating lymphoma from normal LNs ($p < 0.001$).

Correlation analysis

Both elasticity and velocity (r: 0.29) and VI (r: 0.6) values were positively correlated with the volumes of the LNs ($p < 0.001$). There were moderate positive correlations between the VI and elastography parameters [(SWE) (r: 0.5); SI and SWE (r: 0.39); and SI with VI values (0.53) ($p < 0.001$)] (Table 4).

DISCUSSION

Cortical echotexture, spherical shape, capsular irregularity and lack of a fatty hilum of lymph nodes can be reliably investigated using ultrasonography because of its superior geometrical resolution compared to CT and MRI. However, none of these parameters have reached sufficient priority to be a diagnostic parameter alone.[12] Increased acoustic impedance differences between the abnormal LN and surrounding soft tissues have been reported in addition to sharp borders in malignant LNs.[13] However, the hypoechoic appearance of an LN alone, independently from the echogenic hilum and the shape, could not be used to differentiate benign from malignant LNs.[12] As a quantitative parameter of grayscale ultrasonography, the SI, which is calculated as the percent of the shortest to longest diameter ratio, could serve as predictive data for cervical LNs;[14] however, LN diameter alone has been reported as not being able to reach efficient diagnostic performance.[15]

This is the first study to investigate the diagnostic accuracy of VI by SMI combined with SWE for the differential diagnosis of acute inflammatory changes and malignant lymphoma in a pediatric population. In a recent study, microvascular ultrasonography was used to evaluate qualitative vascularity patterns of metastatic lymph nodes and tuberculous lymphadenitis and found to be helpful in differentiation among them.[16] In addition, these quantitative preliminary results can be valuable in terms of normal elasticity parameters of lymph nodes in a healthy pediatric population. SWE values, which are displayed in kPa and m sn^{-1}/, provided efficient diagnostic accuracy in determining lymphoma. Combined evaluation of the LNs with VI could increase diagnostic performance of the grayscale ultrasonography evaluation, especially in acute inflammatory changes.

The vascularity pattern in LNs has been classified as hilar, peripheral-capsular, mixed and avascular.[17] Metastatic LNs and malignant lymphoma have been reported to demonstrate peripheral

Table 3. ROC analysis results by sensitivity, specificity, predictive values and diagnostic accuracy and area under the ROC

Diagnostic performance	Parameter	Cut-off value	Sensitivity (%)	Specificity (%)	PPV (%)	NPV (%)	Diagnostic accuracy (95% CI)	AUC (95% CI)	*p*
Differentiating lymphoma from normal LN	SMI -VI	>15%	91	99	96	94	95 (90–98)	97 (95–99)	0.001
	Elastography parameters	>17 kPa >2.45 m sn^{-1}	96 90	100 99	100 96	99 95	99 (96–99) 95 (46–63)	99 (99–100) 98 (95–100)	0.001 0.001
	SI	>65%	63	100	100	90	91 (86–95)	91 (85–97)	0.001
Differentiating lymphadenitis from normal LN	SMI -VI	>11%	85	84	85	85	85 (78–90)	85 (78–92)	0.001
	Elastography parameters	>2.24 m sn^{-1} >15 kPa	25 27	97 96	82 82	73 74	74 (66–80) 74 (66–80)	61 (51–71) 60 (41–61)	0.01 0.01
	SI	>55%	47	93	78	78	78 (71–84)	75 (65–85)	0.001
Differentiating lymphoma from lymphadenitis	SMI -VI	>15%	85	81	84	82	83 (79–85)	82 (80–85)	0.001
	Elastography parameters	>2.45 m sn^{-1} >17 kPa	96 96	82 81	77 76	98 97	88 (79–99) 87 (78–93)	91 (0–100) 91 (0–100)	0.001 0.001
	SI	>65%	63	70	56	76	68 (57–77)	72 (64–86)	0.002

AUC, area under the curve; LN, lymph node; NPV, negative predictive value; PPV, positive predictive value; ROC, receiver operating characteristic; SI, shape index; SMI, superb microvascular imaging; VI, vascularity index.

vascularity because of neo-angiogenesis and also displaced vessels to the periphery by tumoral infiltration.[18] Vascularity pattern evaluation in combination with grayscale findings have been reported to present a high sensitivity (83%–89%) and specificity (87%–98%) in differentiating malignant from benign LNs.[18] The specific distribution rather than the global increase in Doppler signals would support the limited sensitivity of VI in differentiating lymphoma from lymphadenitis. Power Doppler imaging used for differentiating malignant LNs from benign conditions has revealed that most of the malign LNs present peripheral vascularity with or without central vascularity (92%), and most of the benign LNs exhibit only central vascularity (98%).[19] Although the resistive indices of most of the malignant LNs were reported to be higher than the normal LNs by Ahuja et al, a considerable overlap of the resistive indices among benign and malignant LNs has been reported. In correlation with increased peripheral vascularity in lymphoma, and although the peripheral vascularity is caused by displacement, we demonstrated statistically significant differences among VI values of lymphoma and lymphadenitis groups. In some LNs with a diagnosis of lymphoma, hilar vascularity would decrease because of lymphatic sinusoid obstruction and the deplacement of hilar vessels to the periphery.[17] Thus, overall vascularity would not increase as expected from metastatic diseases. This is why VI was not as efficient as elastography in the lymphoma group and why evaluation of vessel distribution pattern with VI seems to be more specific than VI alone.

Grayscale parameters for indicating lymphoma have been limited. Cut-off values of the shortest diameter for indicating lymphoma higher than 8 mm in cervical LNs has provided diagnostic accuracies of 65%[17] and 84%[8] in previous studies, which has been found to be 11 mm for level 1, 13 mm for level 2, 5 mm for level 3, 9 mm for level 4 and 7 mm for level 5.[8] In routine ultrasonography practice, level 2 and jugulodigastric LNs were commonly encountered stations with LN enlargement. However, normal LNs are less commonly seen in posterior cervical, supraclavicular and the remaining anterior cervical stations. Thus, a fixed cut-off value of shortest diameter alone cannot be applicable for aLNs any station. As far as we know, no available data exist regarding normal cervical LN size based on lymphatic stations and ages as confounding factors in a pediatric population. The SI has been reported to represent an excellent criterion for differentiation between benign and malignant cervical LNs.[14] In addition to considerable diagnostic accuracy in distinguishing lymphoma, the diagnostic accuracy of SI was found to be limited in differentiating lymphadenitis when compared to VI, although the cut-off values were found to be 0.55 for lymphadenitis and 0.65 for lymphoma, which is higher than previous studies. A cut-off value of SI for metastatic LNs was found to be 60% with a diagnostic accuracy of 56%[8] in a recent study, which was 65% for lymphoma with sensitivity, specificity, PPV, NPV and diagnostic accuracy values of 63, 100, 100, 90 and 91%, respectively, in our results. Jugulodigastric LNs presented higher VI values than level 2 cervical LNs in our control group because of the relatively larger hilar vessel diameters and higher LN volumes in jugulodigastric LNs.

Figure 3. ROC analysis of SI, SWE and VI in differentiating lymphadenitis (a) and lymphoma (b) from normal lymph nodes. AUC was 75, 6185 (a) and 91, 98, 97 (b) for SI, SWE and VI, respectively (95% confidence interval). AUC, area under the curve; ROC, receiver operating characteristic; SI, shape index; SWE, shear wave elastography; VI, vascularity index.

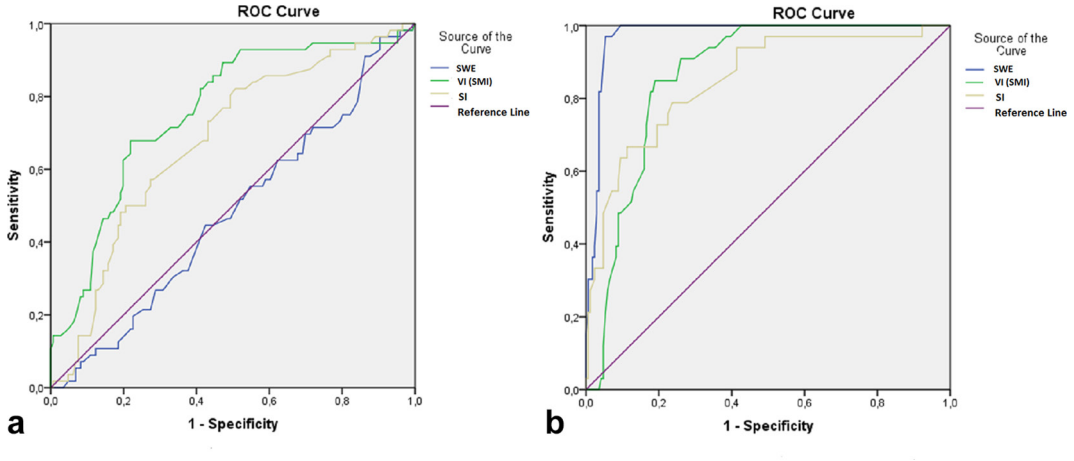

Elastographic evaluation of cervical LNs has been performed in several studies.[8,20–22] Most of them were qualitative or semiquantitative. In the presented study, we expressed the normal values of the LNs' cortical stiffness quantitatively both with kPa and m sn^{-1} and compared the values with benign and malignant LN enlargement. Elastographic parameters did not considerably differ from normal LNs in acute inflammatory processes. Increased VI values in a recently enlarged LN with elasticity values closest to expected for normal LNs would strengthen the diagnosis of lymphadenitis. However, elasticity parameters demonstrated highest diagnostic accuracy for distinguishing lymphoma from lymphadenitis. In a recent study performed with strain elastography, the cut-off value of the strain index of the cervical LNs in comparison with sternocleidomastoid muscle have been reported as 1.18.[23] Based on our results, elasticity values higher than 17 kPa and velocity values higher than 2.45 m sn^{-1} would be considered lymphoma rather than lymphadenitis in an enlarged LN with at least a 91% diagnostic accuracy. In addition, by quantification of the SWE parameters, operator dependence and inter and intraobserver variability will decrease, which makes the examination shorter and the values acceptable and the study reproducible. Evaluation of the LN stiffness in comparison with adjacent soft tissues such as muscles may cause misdiagnosis in cases with overuses, minor injuries, fibromatosis or cerebral palsy.

Our study has some limitations. The sample size in our study was limited, although the study was multicentered, because of the relatively lower incidence of lymphoma. Since histopathological evaluation was performed with the appropriate LN, we included the definite malignant LNs selected based on grayscale ultrasonography findings and confirmed via histopathological evaluation. The ipsilateral subsantimetric LNs hypoechoic than muscles in patients diagnosed with lymphoma were not included. The normal LNs of the patients in the control group were selected among the cervical LNs, and histopathological confirmation was not provided for most of them. LNs located in submandibular regions are generally larger than other lymphatic stations, and based on our findings, they tend to represent higher vascularity[11] in correlation with their volumes. Because of the limited participants, we did not classify the causative agent of lymphadenitis as bacterial or viral or the final histopathological diagnosis as either Hodgkin or non-Hodgkin lymphoma. Therefore, larger series including these subgroups should be evaluated in future studies. Vascularity pattern evaluation along with vascularity indices would exhibit better diagnostic accuracies in differentiating lymphoma from lymphadenitis.

In conclusion, combined grayscale ultrasonography evaluation of LNs with SWE increases the diagnostic power in determining

Table 4. Spearman correlation coefficients (*r*) for variables with *p* values

Parameters	Spearman correlation analysis	
	p value	Rho (*r*)
Age - elasticity and velocity	**0.001**	**0.31**
Age - VI	**0.001**	**0.45**
Age - volume	**0.001**	**0.27**
Shortest diameter - elasticity	**0.001**	**0.40**
Shortest diameter - VI	**0.001**	**0.69**
Longest diameter - VI	**0.001**	**0.38**
Longest diameter - elasticity	0.07	0.1
SI - elasticity	**0.001**	**0.39**
SI - VI	**0.001**	**0.53**
Volume - elasticity and velocity	**0.001**	**0.29**
Volume - VI	**0.001**	**0.6**
Elasticity - VI	**0.001**	**0.5**
Peripheral vascularity - shortest diameter	**0.001**	**0.64**
Peripheral vascularity - elasticity	**0.001**	**0.5**
Peripheral vascularity - VI	**0.001**	**0.67**

SI, shape index; VI, vascularity index.

lymphoma. Multimodality evaluation of lymph nodes by addition of VI via SMI provides the best diagnostic performance in distinguishing lymphadenitis and also VI is efficient in diagnosing malignant lymphoproliferative disorders.

ETHICAL APPROVAL

This article does not contain any studies with animals performed by any of the authors. All procedures performed in studies involving human participants were in accordance with the ethical standards of the institutional research committee and with the 1964 Helsinki declaration and its later amendments or comparable ethical standards.

INFORMED CONSENT

Informed consent was obtained from all individual participants included in the study.

REFERENCES

1. Shirakawa T, Miyamoto Y, Yamagishi J, Fukuda K, Tada S. Color/power Doppler sonographic differential diagnosis of superficial lymphadenopathy: metastasis, malignant lymphoma, and benign process. *J Ultrasound Med* 2001; **20**: 525–32. doi: https://doi.org/10.7863/jum.2001.20.5.525
2. Lee YS, Kim MJ, Han SW, Lee HS, Im YJ, Shin HJ, et al. Superb microvascular imaging for the detection of parenchymal perfusion in normal and undescended testes in young children. *Eur J Radiol* 2016; **85.3**: 649–56. doi: https://doi.org/10.1016/j.ejrad.2015.12.023
3. Machado P, Segal S, Lyshchik A, Forsberg F. A novel microvascular flow technique: initial results in thyroids. *Ultrasound Q* 2016; **32**: 67–74. doi: https://doi.org/10.1097/RUQ.0000000000000156
4. Ohno Y, Fujimoto T, Shibata Y. A new era in diagnostic ultrasound, superb microvascular imaging: preliminary results in pediatric hepato-gastrointestinal disorders. *Eur J Pediatr Surg* 2017; **27**: 020–5. doi: https://doi.org/10.1055/s-0036-1593381
5. Xiao XY, Chen X, Guan XF, Wu H, Qin W, Luo BM. Superb microvascular imaging in diagnosis of breast lesions: a comparative study with contrast-enhanced ultrasonographic microvascular imaging. *Br J Radiol* 2016; **89**: 20160546. doi: https://doi.org/10.1259/bjr.20160546
6. Săftoiu A, Vilmann P, Hassan H, Gorunescu F. Analysis of endoscopic ultrasound elastography used for characterisation and differentiation of benign and malignant lymph nodes. *Ultraschall Med* 2006; **27**: 535–42. doi: https://doi.org/10.1055/s-2006-927117
7. Lyshchik A, Higashi T, Asato R, Tanaka S, Ito J, Hiraoka M, et al. Cervical lymph node metastases: diagnosis at sonoelastography-initial experience. *Radiology* 2007; **243**: 258–67. doi: https://doi.org/10.1148/radiol.2431052032
8. Alam F, Naito K, Horiguchi J, Fukuda H, Tachikake T, Ito K. Accuracy of sonographic elastography in the differential diagnosis of enlarged cervical lymph nodes: comparison with conventional B-mode sonography. *AJR Am J Roentgenol* 2008; **191**: 604–10. doi: https://doi.org/10.2214/AJR.07.3401
9. Aoyagi S, Izumi K, Hata H, Kawasaki H, Shimizu H. Usefulness of real-time tissue elastography for detecting lymph-node metastases in squamous cell carcinoma. *Clin Exp Dermatol* 2009; **34**: e744–e747. doi: https://doi.org/10.1111/j.1365-2230.2009.03468.x
10. Ying L, Hou Y, Zheng HM, Lin X, Xie ZL, Hu YP, . Real-time elastography for the differentiation of benign and malignant superficial lymph nodes: a meta-analysis. *Eur J Radiol* 2012; **81**: 2576–84. doi: https://doi.org/10.1016/j.ejrad.2011.10.026
11. Ying M, Ahuja AT. Ultrasound of neck lymph nodes: how to do it and how do they look? *Radiography* 2006; **12**: 105–17. doi: https://doi.org/10.1016/j.radi.2005.04.004
12. Dudea SM, Lenghel M, Botar-Jid C, Vasilescu D, Duma M. Ultrasonography of superficial lymph nodes: Benign vs. malignant. *Med Ultrasonogr* 2012; **14**: 294.
13. Ahuja AT, Ying M, Ho SY, Antonio G, Lee YP, King AD, et al. Ultrasound of malignant cervical lymph nodes. *Cancer Imaging* 2008; **8**: 48–56. doi: https://doi.org/10.1102/1470-7330.2008.0006
14. Steinkamp HJ, Cornehl M, Hosten N, Pegios W, Vogl T, Felix R. Cervical lymphadenopathy: ratio of long- to short-axis diameter as a predictor of malignancy. *Br J Radiol* 1995; **68**: 266–70. doi: https://doi.org/10.1259/0007-1285-68-807-266
15. Sumi M, Ohki M, Nakamura T. Comparison of sonography and CT for differentiating benign from malignant cervical lymph nodes in patients with squamous cell carcinoma of the head and neck. *AJR Am J Roentgenol* 2001; **176**: 1019–24. doi: https://doi.org/10.2214/ajr.176.4.1761019
16. Ryoo I, Suh S, You SH, Seol HY. Usefulness of microvascular ultrasonography in differentiating metastatic lymphadenopathy from tuberculous lymphadenitis. *Ultrasound Med Biol* 2016; **42**: 2189–95. doi: https://doi.org/10.1016/j.ultrasmedbio.2016.05.012
17. Ahuja A, Ying M. Sonographic evaluation of cervical lymphadenopathy: is power Doppler sonography routinely indicated? *Ultrasound Med Biol* 2003; **29**: 353–9. doi: https://doi.org/10.1016/S0301-5629(02)00759-7
18. Ahuja A, Ying M. Sonography of neck lymph nodes. Part II: abnormal lymph nodes. *Clin Radiol* 2003; **58**: 359–66. doi: https://doi.org/10.1016/S0009-9260(02)00585-8
19. Ahuja AT, Ying M, Ho SS, Metreweli C. Distribution of intranodal vessels in differentiating benign from metastatic neck nodes. *Clin Radiol* 2001; **56**: 197–201. doi: https://doi.org/10.1053/crad.2000.0574
20. Bhatia KS, Cho CC, Yuen YH, Rasalkar DD, King AD, Ahuja AT. Real-time qualitative ultrasound elastography of cervical lymph nodes in routine clinical practice: interobserver agreement and correlation with malignancy. *Ultrasound Med Biol* 2010; **36**: 1990–7. doi: https://doi.org/10.1016/j.ultrasmedbio.2010.08.016
21. Zaleska-Dorobisz U, Pawluś A, Szymańska K, Łasecki M, Ziajkiewicz M. Ultrasound elastography-review of techniques and its clinical applications in pediatrics-part 2. *Adv Clin Exp Med* 2015; **24**: 725–30. doi: https://doi.org/10.17219/acem/34581
22. Nazarian LN. Can sonoelastography enable reliable differentiation between benign and metastatic cervical lymph nodes? *Radiology* 2007; **243**: 1–2. doi: https://doi.org/10.1148/radiol.2431061626
23. Turgut E, Celenk C, Tanrivermis Sayit A, Bekci T, Gunbey HP, Aslan K. Efficiency of B-mode ultrasound and strain elastography in differentiating between benign and malignant cervical lymph nodes. *Ultrasound Q* 2017; **33**: 201–7. doi: https://doi.org/10.1097/RUQ.0000000000000302